Journal of Peptide Science
J. Peptide Sci. **11**: 379–389 (2005)
Published online 20 December 2004 in Wiley InterScience (www.interscience.wiley.com). DOI: 10.1002/psc.629

JOURNAL OF PEPTIDE SCIENCE

Structural studies and model membrane interactions of two peptides derived from bovine lactoferricin

LEONARD T. NGUYEN, DAVID J. SCHIBLI‡ and HANS J. VOGEL*

Structural Biology Research Group, Department of Biological Sciences, University of Calgary, Calgary, Alberta, T2N 1N4 Canada

Received 23 July 2004; Accepted 1 October 2004

Abstract: The powerful antimicrobial properties of bovine lactoferricin (LfcinB) make it attractive for the development of new antimicrobial agents. An 11-residue linear peptide portion of LfcinB has been reported to have similar antimicrobial activity to lactoferricin itself, but with lower hemolytic activity. The membrane-binding and membrane-perturbing properties of this peptide were studied together with an amidated synthetic version with an added disulfide bond, which was designed to confer increased stability and possibly activity. The antimicrobial and cytotoxic properties of the peptides were measured against *Staphylococcus aureus* and *Escherichia coli* and by hemolysis assays. The peptides were also tested in an anti-cancer assay against neuroblastoma cell lines. Vesicle disruption caused by these LfcinB derivatives was studied using the fluorescent reporter molecule calcein. The extent of burial of the two Trp residues in membrane mimetic environments were quantitated by fluorescence. Finally, the solution NMR structures of the peptides bound to SDS micelles were determined to provide insight into their membrane bound state. The cyclic peptide was found to have greater antimicrobial potency than its linear counterpart. Consistent with this property, the two Trp residues of the modified peptide were suggested to be embedded deeper into the membrane. Although both peptides adopt an amphipathic structure without any regular α-helical or ß-sheet conformation, the 3D-structures revealed a clearer partitioning of the cationic and hydrophobic faces for the cyclic peptide.

Keywords: antimicrobial peptide; bovine lactoferricin; disulfide induced circularization; micelle-bound structure; nuclear magnetic resonance; peptide–membrane interactions; steady-state fluorescence spectroscopy

INTRODUCTION

Lactoferricin is a 25-residue disulfide cross-linked peptide released by gastric pepsin proteolytic cleavage from the *N*-terminus of lactoferrin, an 80 kDa iron-binding glycoprotein found in milk and other exocrine secretions [1,2]. This peptide has been shown to have markedly increased antimicrobial properties over its uncleaved counterpart [2]. Comparisons of homologues including the human, caprine, murine and porcine lactoferricins have found bovine lactoferricin (LfcinB) to have a higher bactericidal potency [3,4], making the latter a particularly attractive target for antimicrobial drug development.

A hexamer section (RRWQWR-NH_2) of LfcinB containing an amidated *C*-terminus has been shown to display antimicrobial activity comparable to the full peptide [5]. This region has been termed the 'antimicrobial center' of lactoferricin B. Also, an 11-residue segment encompassing this center (RRWQWRMKKLG) was found to have similar antimicrobial performance while showing reduced hemolytic activity compared with the intact peptide [6]. This segment is particularly attractive because of its apparent loss of toxicity against mammalian cells. Studies concentrating on the Trp residues have shown that they are crucial for the antimicrobial activity [3]. Additionally, a comparison between LfcinB and human lactoferricin, which contains only one Trp instead of two, reveals that there is a 'Trp effect' that plays a part in enhancing the antimicrobial effectiveness [7].

In the light of the growing interest in producing antimicrobial peptides with clinical potency to combat multidrug resistant bacteria [8], the previously studied 11-residue peptide [6] was modified in the hope of creating a potent antimicrobial agent with enhanced structural stability. Here, the 11-mer, termed $LfcinB_{4-14}$, has been studied in comparison with another peptide containing the same 11 residues flanked by a Cys residue on each terminus that are linked to each other through a disulfide bond. The *N*-terminal Cys of this peptide is already present in LfcinB. Native LfcinB also includes a disulfide link, although it is between two

Abbreviations: COSY, correlation spectroscopy; DPC, dodecylphosphatidylcholine; DSS, 2,2-dimethyl-2-silapentane-5-sulphonic acid; ePC, egg α-phosphatidylcholine; ePE, egg α-phosphatidylethanolamine; ePG, egg α-phosphatidylglycerol; ESI-MS, electrospray ionization mass spectrometry; HPLC, high-performance liquid chromatography; LfcinB, bovine lactoferricin; LUV, large unilamellar vesicle; K_{SV}, Stern-Volmer constant; MBC, minimum bactericidal concentration; MIC, minimum inhibitory concentration; NMR, nuclear magnetic resonance; NOE, nuclear Overhauser enhancement; NOESY, nuclear Overhauser effect spectroscopy; PC, phosphatidylcholine; PE, phosphatidylethanolamine; PG, phosphatidylglycerol; rmsd, root mean square deviation; SDS, sodium dodecyl sulphate; TOCSY, total correlation spectroscopy.

*Correspondence to: Dr Hans J. Vogel, Department of Biological Sciences, University of Calgary, Calgary, Alberta, T2N 1N4 Canada; e-mail: vogel@ucalgary.ca
‡ Current address: European Molecular Biology Laboratories, Grenoble Outstation, Grenoble, 38042 France.

more sequentially distant Cys residues. The original cross-link has been found to have little effect on antimicrobial activity [9,10]. The *C*-terminus of the cyclized peptide has also been amidated to improve the overall cationic nature of the peptide, a modification strategy previously used on other synthetic LfcinB-based peptides [3]. This second peptide, termed $LfcinB_{4-14}$Disu, has the final sequence CRRWQWRMKKLGC-NH_2. These modifications were made to give the 11-residue segment greater protease stability while being bound to bacterial membranes, thereby creating a peptide with potentially greater efficiency in antimicrobial activity. A similar approach has led to the successful design of a stable derivative of indolicidin, another antimicrobial peptide with multiple Trp residues, with increased potency and protease stability [11].

It has often been suggested that most antimicrobial peptides act solely through membrane interactions [12]. However, some of these peptides have been shown to enter the cell where they bind to intracellular targets to cause their effects [13,14]. Regardless of these different mechanisms, one of the initial sites of interaction for these cationic peptides is with the plasma membrane [15,16]. In particular, the cell envelope seems to be the limiting step for the full LfcinB to exert its antimicrobial effect [17]. The interactions with various bacterial membrane models were studied by fluorescence spectroscopy. Bacterial membranes are negatively charged because they are mainly composed of the zwitterionic PE and the anionic PG lipids. This net charge provides the main attractant for cationic antimicrobial peptides. The outer leaflets of eukaryotic membranes, on the other hand, are neutral because they are primarily composed of zwitterionic PC. Net negatively charged large unilamellar vesicles (LUV) composed of 1 : 1 ratios of PE : PG and PC : PG lipids from chicken egg sources, believed to represent a good variety of bacterial fatty acyl tails, were used for our studies. Specifically, the amount of leakage of intravesicular contents caused by the peptides was determined using a soluble fluorescent reporter molecule. In addition, the burial of the Trp residues of the peptides within the bilayer was probed by measuring indole fluorescence. As a control, the same experiments were performed using PE : PC LUVs to represent neutrally charged membranes that are characteristic for eukaryotic membranes. NMR spectra of these peptides bound to SDS micelles were then acquired allowing their 3D-structures to be solved.

MATERIALS AND METHODS

Materials

$LfcinB_{4-14}$ and $LfcinB_{4-14}$Disu were synthesized by the Peptide Synthesis Facility at the University of Western Ontario, London, Canada, as described by Brewer and Lajoie [18] using Fmoc chemistry on Wang resin [19]. Arginine was protected with pentamethylchromane-6-sulfonyl, cysteine was protected with the trityl group, and lysine was protected as the *tert*-butyloxycarbonyl group. The two Cys residues of the crude $LfcinB_{4-14}$Disu peptide (0.5 mg/ml) were air oxidized in a 0.1 M deaerated solution of ammonium bicarbonate to form an intramolecular disulfide bond. Subsequently, the peptides were purified by semi-preparative reversed phase HPLC. Purities of at least 95% were determined by analytical HPLC with additional identity and purity confirmations by ESI-MS. Peptide concentrations were determined by UV absorbance at 280 nm and theoretically determined extinction coefficients of $\varepsilon(280)_{LfcinB4-14}$ of 11 380 M^{-1} cm^{-1} and $\varepsilon(280)_{LfcinB4-14Disu}$ of 11 500 M^{-1} cm^{-1}.

All phospholipids were obtained from Avanti Polar Lipids (Alabaster, AL). For preparation of LUVs, the ingredients were as follows: the sodium salt of ePG; chicken ePE; and ePC. The phospholipids received were dissolved in chloroform.

Biological Activity Assays

All biological activity assays were carried out in triplicate at the University Hospital in Tromsø, Norway. MIC and MBC assays were performed on the two peptides as well as an amidated version of $LfcinB_{4-14}$ ($LfcinB_{4-14}$-NH_2) according to Ulvatne *et al.* [20] using *Escherichia coli* (*E. coli*) ATCC25922 and *Staphylococcus aureus* (*S. aureus*) ATCC25923. Briefly, a standard microdilution in 1% bacto peptone water was used as previously described by Vorland *et al.* [4]. The MBC was determined by the peptide concentration reducing the colony forming units of overnight-grown agar plates by 99%.

Hemolytic concentration assays were performed according to Strom *et al.* [21]. Briefly, erythrocytes were isolated from heparinized human blood by centrifugation after three washes with phosphate-buffered saline (5 mM phosphate buffer, 150 mM NaCl, pH 7.4). Different peptide concentrations were incubated with aliquots containing 10^7 cells/ml for 30 min at 37 °C with gentle mixing. After centrifugation, the A_{540} values of the resulting supernatants were measured. Zero hemolysis (blank) and 100% hemolysis were determined in phosphate buffer and 1% Triton X-100, respectively, and concentrations causing 50% hemolysis were determined from the dose-response curves.

For comparison, the same assays were also performed with tritrpticin, an antimicrobial peptide of the same Trp-rich peptide family [22].

Finally, toxicity assays were carried out according to Eliassen *et al.* [23] against neuroblastoma cell lines. Briefly, a 4 h incubation at 37 °C in serum-free culture was followed by the microtetrazolium-based colorimetric assay [24]. The concentrations with 50% cell survival were determined from the dose-response curves.

Preparation of Large Unilamellar Vesicles

The LUV preparations were adapted from Schibli *et al.* [22], with relevant details and amendments as described here. The vesicles were prepared from 1 : 1 mixtures of ePC : ePG, ePE : ePG and ePE : ePC lipids. Solvent evaporation was achieved under a stream of nitrogen gas followed by incubation in a vacuum chamber for 1–2 h. The remaining film was suspended by vortexing in a Tris buffer (10 mM Tris, 150 mM

NaCl, 1 mM EDTA, pH 7.4). The lipid suspensions were further processed with five cycles of freezing and thawing followed by 15 passes through two stacked 0.1 μm polycarbonate filters (Nucleopore Filtration Products, Pleasanton, CA) using a mini-extruder (Avanti Polar Lipids) at room temperature [25,26]. Lipid phosphorus concentrations of the finished vesicles were determined by the Ames method [27] with subtraction of phosphorus in control buffer blanks.

The preparation of calcein encapsulated LUV was adapted from Matsuzaki *et al.* [28]. These LUVs were made in the same Tris buffer used for fluorometric assays with the addition of 70 mM calcein. Following LUV extrusion, free calcein was removed by gel-filtration on a G50 Superfine 15 cm column running calcein-free Tris buffer. Fractions containing the calcein encapsulated vesicles were detected by absorption at a wavelength of 400 nm and recovered.

Steady-State Fluorescence Studies

All fluorescence measurements were done in triplicate with a Varian Cary Eclipse fluorimeter, with a temperature controller attachment to keep the samples at 37 °C. All sample volumes were 2 ml using the Tris buffer, pH 7.4, for dilutions.

Calcein Fluorescence: LUV Leakage Assays

For this assay, a method in the Varian Kinetics program was used with excitation settings at 490 nm with a slit width of 5 nm and emission detection at 520 nm with a slit width of 5 nm. This method was adapted from Matsuzaki *et al.* [28]. At a 10 : 1 lipid : peptide ratio, a baseline reading of 10 μM of calcein encapsulated vesicles (ePC : ePG, ePE : ePG or ePE : ePC) was taken for 1 min, whereupon the peptide, either $LfcinB_{4-14}$Disu or $LfcinB_{4-14}$, was added to a 1 μM concentration. Calcein leakage due to the peptide addition was monitored for 5 min. Maximal vesicle leakage was then measured by the addition of the detergent Triton X-100 from a 10% stock solution to a final concentration of 0.1% v/v concentration and monitoring for a further 1.5 min period on the same kinetic run. Control runs were done with the related antimicrobial peptide, tritrpticin. Calculation of calcein leakage, % *leakage*, was done as follows:

$$\%\ leakage = 100 \times (I - I_o)/(I_t - I_o),$$

where I is the fluorescence intensity 5 min after peptide addition, I_o is the intensity after 1 min of intact vesicle baseline acquisition, and I_t is the intensity 1.5 min after the addition of Triton X-100.

Tryptophan Fluorescence: Blue Shift Effect and Acrylamide Quenching

Tryptophan fluorescence experiments were adapted from Schibli *et al.* [22], with relevant details and amendments as described here. The Varian Scan program was used with excitation settings at 280 nm with a slit width of 10 nm and emission detection from 300 to 400 nm with a slit width of 10 nm. Measurements were made on 1 μM of test peptide in the following membrane-mimetic environments: 30 μM ePC : ePG LUVs, 30 μM ePE : ePG LUVs, 30 μM ePE : ePC LUVs, 25 mM SDS, 25 mM DPC, and a blank control (Tris, pH 7.4 buffer alone). As an extension of the blue shift studies, acrylamide quenching titrations from a 4.0 M stock solution were done incrementally on samples to a final acrylamide concentration of 0.1 M.

The K_{SV} constants [29] were determined from

$$Fo/F = 1 + K_{SV}[Q]$$

where Fo is the initial fluorescence of the peptide with no acrylamide added, F is the fluorescence of the peptide in the presence of various concentrations of acrylamide, and $[Q]$ is the concentration of acrylamide.

NMR Sample Preparation

3 mM $LfcinB_{4-14}$ and 2 mM $LfcinB_{4-14}$Disu NMR samples were produced by dissolving lyophilized peptide powder in 90% H_2O/10% D_2O. As NMR signals would be too broad due to the large correlation time of the peptide-bound vesicle complexes, SDS micelles were used as a suitable membrane-mimic in lieu of LUVs [16]. An SDS : peptide ratio of at least 60 : 1 was used and the chemical shift reference compound DSS was added to the samples. Final pH adjustments were made to 4.4 for the $LfcinB_{4-14}$ sample and 4.2 for the $LfcinB_{4-14}$Disu sample.

NMR Spectroscopy

Two-dimensional NOESY, TOCSY (mixing times of 100 ms and 60 ms, respectively) and COSY spectra were acquired at 25 °C and 37 °C for the $LfcinB_{4-14}$ and $LfcinB_{4-14}$Disu samples on a Bruker Avance 700 MHz NMR spectrometer and a Bruker Avance 500 MHz NMR spectrometer equipped with a Cryo-probe™. All spectra from the 700 MHz spectrometer were acquired with 4096 × 1024 data points in the *F2* and *F1* dimensions, and sweep widths of 10 964.912 Hz. The spectra from the 500 MHz spectrometer were acquired with 2048 × 600 (4096 × 600 for the COSYs) data points in the *F2* and *F1* dimensions, and sweep widths of 7002.801 Hz (6009.615 Hz for the COSYs). In all NOESY and TOCSY spectra, water suppression was achieved using excitation sculpting [30], while Watergate [31] was used in the COSYs. All spectra were zero-filled and multiplied by a shifted sine-bell curve using the NMRPipe software package [32].

Structure Calculations

NMR spectra were analysed using NMRView 5.0.3 [33] on workstations running the Redhat 7.1 version of the Linux operating system. All NMR spectra were initially referenced to DSS at 0.00 ppm. The assignment of the protein chemical shifts was determined using the method of Wüthrich [34]. Initial protein structures were generated from extended structures using the program CNS (version 1.0) [35]. Due to the disulfide bond in the $LfcinB_{4-14}$Disu peptide, a simulated annealing and molecular dynamics protocol was used to produce low energy structures with the minimum distance and geometry restraint violations for the cyclized peptide. Otherwise, the default parameters supplied with the program were used. The peptide structures were further refined using the program ARIA (version 1.2) [36] on a Linux workstation. ARIA features the incorporation of ambiguous NOE distance restraints into the structure calculations as well as the

calibration of the NOE distance restraints using a structure-based NOE back-calculation. In the final ARIA run, the number of structures generated in the ninth iteration was increased to 100, and 20 structures were kept based on lowest energy.

RESULTS

Antimicrobial, Hemolytic and Anti-cancer Activity

$LfcinB_{4-14}Disu$ was found to perform better in both MIC and MBC assays than $LfcinB_{4-14}$ using both the Gram-negative *E. coli* and the Gram-positive *S. aureus* (Table 1). Both peptides were more cytotoxic against *E. coli* than against *S. aureus*. The results obtained with the amidated version of $LfcinB_{4-14}$ show that, especially against *E. coli*, the increased activity arises mostly from the disulfide bond. However, the cyclic peptide was found to be slightly less active than the control tritrpticin peptide. Within detectable limits, hemolysis data showed the Lfcin-derived peptides to be greatly non-toxic to erythrocytes, whereas tritrpticin showed some toxicity. Intact lactoferricin, but not its linearized version, also had a potent activity against various cancer cell lines and mouse tumors [23]. Therefore the potencies of both the linear and the cyclic peptide were tested against neuroblastoma cell lines: both were poor anti-cancer peptides (Table 2), especially compared with native LfcinB.

LUV Lysis Assays

To study the membrane disruption properties of the peptides, the release of the fluorescent reporter molecule calcein was measured over a period of time upon addition of peptide. Calcein is self-quenching at high concentrations, and so its fluorescence will increase upon release from vesicles and subsequent dilution [20]. The leakage results obtained at a 10 : 1 lipid : peptide ratio are shown in Figure 1A, with sample kinetic runs shown on the B panel for ePC : ePG LUVs. Assays at greater lipid : peptide ratios were performed but are not shown because the leakage was already very low at the 10 : 1 ratio. In general, a very small increase in calcein fluorescence was observed upon addition of either of the LfcinB derived peptides to both ePC : ePG and ePE : ePG LUVs, compared with tritrpticin. Slightly more leakage was induced by the peptides on ePC : ePG surfaces than ePE : ePG LUVs. The leakage profile for $LfcinB_{4-14}$ showed that it consistently caused lower amounts of leakage than the cyclic peptide. However, this difference is within the uncertainties of the data, due to the low intensities of calcein fluorescence recorded. While there was considerable leaking of the ePE : ePC LUVs by tritrpticin, both Lfcin-derived peptides showed almost no leakage from these vesicles containing the zwitterionic phospholipid head groups.

Table 1 Inhibitory, Bactericidal and Hemolysis Assays

Peptide	*E. coli*		*S. aureus*		Hemolysis
	MIC (μg/ml)	MBC (μg/ml)	MIC (μg/ml)	MBC (μg/ml)	EC_{50} (μg/ml)
$LfcinB_{4-14}$	50	50	100–150	200	>1000
$LfcinB_{4-14}$ Disu	20	25–50	25–50	50	>1000
$LfcinB_{4-14}$-NH_2	30–40	60–70	30–50	70–90	>1000
Tritrpticin	20	20	10–20	20	380

Table 2 Biological Activities against Neuroblastoma Cell Lines

Peptide	IC_{50} (μg/ml)
$LfcinB_{4-14}$	>500
$LfcinB_{4-14}Disu$	>500
LfcinB (native)	30

Blue Shift of Trp Residues

The environments of the two Trp residues of the peptides when bound to a membrane can be measured by the blue shift in the fluorescence emission spectrum as a consequence of the Trp residue being exposed to the hydrophobic environment from the fatty acyl tails of the lipids. This shift to shorter maximum emission wavelengths from 357 nm and 352 nm for $LfcinB_{4-14}$ and $LfcinB_{4-14}Disu$, respectively, in the reference aqueous buffer was observed in the presence of the ePE : ePG and ePC : ePG LUVs, with a more pronounced effect seen in the ePE : ePG vesicles (Table 3). Also, SDS and DPC micelles provided more hydrophobic environments for the Trp residues. All four of these membrane-mimetic environments, especially SDS micelles, show the Trp residues of the cyclic LfcinB-derived peptide to be within a more hydrophobic environment than $LfcinB_{4-14}$. The fluorescence results with ePE : ePC LUVs, on the other hand, do not show any blue shift when either peptide is introduced.

Quenching of Trp Fluorescence

As a complement to the blue shift measurements, the extent of burial of the Trp residues into different hydrophobic environments was examined further by measuring the Stern-Volmer constants for each of the peptides as a result of quenching by acrylamide. As a Trp fluorophore becomes embedded into a vesicle or micelle, it loses its exposure to the solvent and so its fluorescent properties are less affected by a titrated soluble quencher. The greater the protection

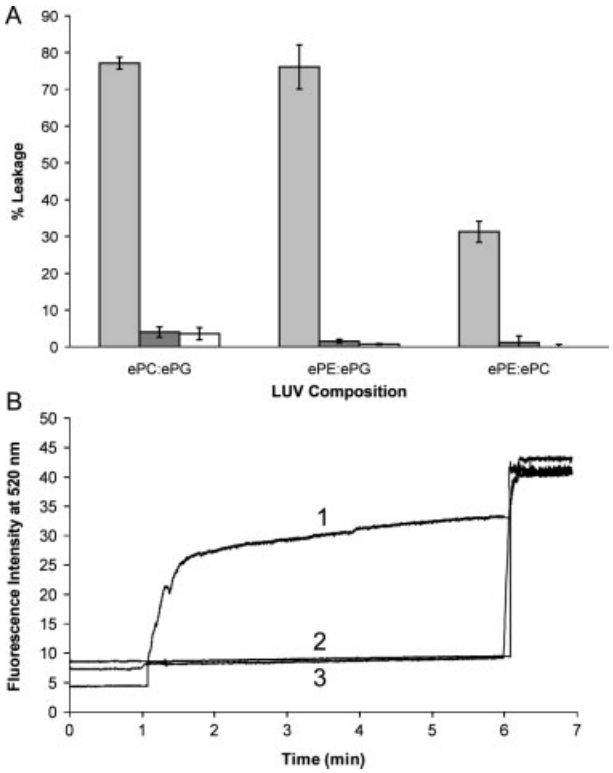

Figure 1 LUV leakage assays based on calcein fluorescence. (A) The amount of intravesicular leakage upon the addition of tritrpticin (light grey), LfcinB$_{4-14}$ (blank) and LfcinB$_{4-14}$Disu (dark grey) at a peptide : lipid ratio of 1 : 10 for vesicles of different lipid composition. Calcein-encapsulated LUV and peptide concentrations remained constant Tris, pH 7.4, for every run. Each data point represents the average of three measurements at 37 °C. (B) One sample leakage run for tritrpticin (1), LfcinB$_{4-14}$ (2), and LfcinB$_{4-14}$Disu (3) added to ePC : ePG LUVs.

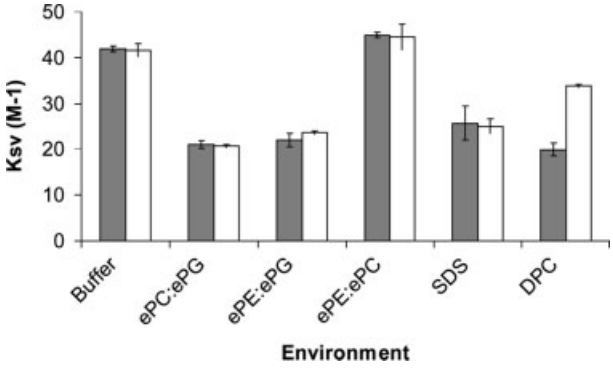

Figure 2 Stern-Volmer (K_{sv}) constants of LfcinB$_{4-14}$ (blank) and LfcinB$_{4-14}$Disu (dark grey) in different membrane mimetic environments as determined from acrylamide quenching experiments.

of the Trp residues, the smaller the K_{sv}. Acrylamide was used as the quencher because it is neutral and uncharged. Due to concerns of having free peptides, that is peptides that are unbound to any vesicle or micelle and hence free to be maximally quenched by acrylamide, an excess of the vesicle or micelle was used in these experiments.

The results from these experiments are shown in Figure 2. The ePE : ePC results show that the Trp residues of both peptides are roughly as accessible to the quencher as in the buffer alone, suggesting little interaction of these vesicles with the peptides. The results obtained for the two peptides in DPC micelles show a greatly different profile when compared with the results with SDS micelles and ePG containing LUVs. With DPC introduced as a binding partner, the Trp residues of LfcinB$_{4-14}$ are more exposed to the aqueous solvent compared with the disulfide-bonded peptide. The SDS micelle environment gives less acrylamide quenching of the Trp residues than do the LUVs. In experiments with the ePG containing LUVs, increased segregation of the Trp residues away from the solvent is seen slightly more with ePC : ePG surfaces compared with ePE : ePG surfaces. A comparison shows that with all LUV types and SDS micelles, there is no great difference in solvent exposure of the Trp residues between the disulfide-linked peptide and its linear counterpart.

Structural Calculations

The structures of the micelle-bound peptides were determined at 37 °C over those at 25 °C because the higher temperature structures showed greater agreement with each other. Table 4 displays the structural statistics for the final 20 NMR structures generated by ARIA for both peptides.

The 3D structures obtained for LfcinB$_{4-14}$ are shown in Figures 3A and 3C. The respective global rmsd for the backbone and heavy atoms are 0.232 Å and 0.786 Å for residues 2–10 of LfcinB$_{4-14}$, while these

Table 3 Blue Shifts in Maximum Emission Wavelength of Tryptophan Fluorescence

Peptide	Reference wavelength in buffer (nm)	Shifts (nm)				
		ePC : ePG	ePE : ePG	ePE : ePC	SDS	DPC
LfcinB$_{4-14}$	357	3	5	−2	9	10
LfcinB$_{4-14}$Disu	352	7	9	0	17	12

values are 0.577 Å and 1.025 Å for residues of the full peptide. A glance at the structures reveals that a major contribution to the difference in rmsd values between residues 2–10 and 1–11 is from the two main conformations for the floppy *C*-terminal Gly11. The final 20 structures of this peptide contain no regular secondary structure pattern, as exemplified in Figures 4A and 4C, which show one of the final structures with highlighted residues. There are sharp bends through the Met7-Lys8-Lys9-Leu10 residues so that the positive residues of this sequence fall on one side while the hydrophobic residues lie on the other side. Furthermore, all the residues with side-chains considered to have a significant degree of hydrophobicity, that is Trp3, Trp5, Met7 and Leu10, are in line with each other (Figure 4A), with the planar aromatic planes of the Trp residues lying parallel to each other and perpendicular to their immediate backbone. The Trp residues are mostly defined to be in the interior of the peptide rather than protruding outward as do Met7 and Leu10. The five positive side-chains of the Arg and Lys residues all extend themselves out of the backbone at various angles to form somewhat of a positive cloud to cover the other residues in $LfcinB_{4-14}$ (Figure 4C).

The $LfcinB_{4-14}$Disu structures (Figures 3B and 3D) have a global rmsd for the backbone and heavy atoms of 0.324 Å and 0.862 Å, respectively, for residues 2–12, while these values do not change greatly when considering the full peptide (0.372 Å and 0.862 Å). These values show that the introduced cystine bond gives the entire $LfcinB_{4-14}$Disu a more defined structure compared with $LfcinB_{4-14}$. Due to the constraints of the disulfide link between such proximal Cys residues, a number of lesser-favored angles are found in the structure, making the angular rmsd from ideal values relatively high. In addition, the percentages of the regions of the Ramachandran map [37], as determined by the Procheck program [38] have fewer residues residing in the most favored classification and more toward the additionally allowed group. Like the $LfcinB_{4-14}$ peptide, the $LfcinB_{4-14}$Disu backbone shows no regular secondary structure (Figures 4B and 4D), although there appears to be an α-turn-like conformation [39] for residues 5–8. The lack of

Table 4 Structural Statistics for the Final 20 NMR Structures of $LfcinB_{4-14}$ and $LfcinB_{4-14}$Disu

	$LfcinB_{4-14}$	$LfcinB_{4-14}$Disu
No. of distance restraints[a]		
Unambiguous NOEs	287	436
Ambiguous NOEs	14	22
Unassigned NOEs	0	0
Total NOEs	301	731
rmsd from ideal values		
Bonds (Å)	$1.78 \times 10^{-3} \pm 1.05 \times 10^{-4}$	$2.12 \times 10^{-3} \pm 3.40 \times 10^{-5}$
Angles (degree)	$0.36 \pm 1.46 \times 10^{-2}$	$0.41 \pm 2.66 \times 10^{-2}$
Impropers (degree)	$0.21 \pm 2.62 \times 10^{-2}$	$0.21 \pm 2.12 \times 10^{-2}$
van der Waals (kcal/mol)	15.40 ± 0.57	15.73 ± 1.16
Distance restraints		
Unambiguous (Å)	$6.37 \times 10^{-2} \pm 4.08 \times 10^{-2}$	$7.71 \times 10^{-2} \pm 4.51 \times 10^{-2}$
Ambiguous (Å)	$1.52 \times 10^{-2} \pm 7.64 \times 10^{-3}$	$2.28 \times 10^{-2} \pm 1.46 \times 10^{-2}$
All distance restraints (Å)	$0.11 \pm 2.96 \times 10^{-2}$	$9.70 \times 10^{-2} \pm 2.80 \times 10^{-2}$
Dihedral restraints (degree)	0.40 ± 0.12	0.04 ± 0.04
Non-bonded energies		
Electronic (kcal/mol)	-74.13 ± 48.62	-93.13 ± 38.07
van der Waals (kcal/mol)	-75.80 ± 31.07	-185.35 ± 81.44
Regions of Ramachandran map [37] (%)[b]		
Most favored	37.8	24.5
Additionally allowed	26.1	47.5
Generously allowed	36.1	28.0
Disallowed	0.0	0.0
Global rmsd (Å)[c]		
Backbone	0.232/0.577	0.324/0.372
Heavy atom	0.786/1.025	0.862/0.862

[a] From the final ARIA iteration.
[b] As determined by Procheck [38].
[c] Calculated by MOLMOL [50] for residues 2–10/1–11 and residues 2–12/1–13 for $LfcinB_{4-14}$ and $LfcinB_{4-14}$Disu, respectively.

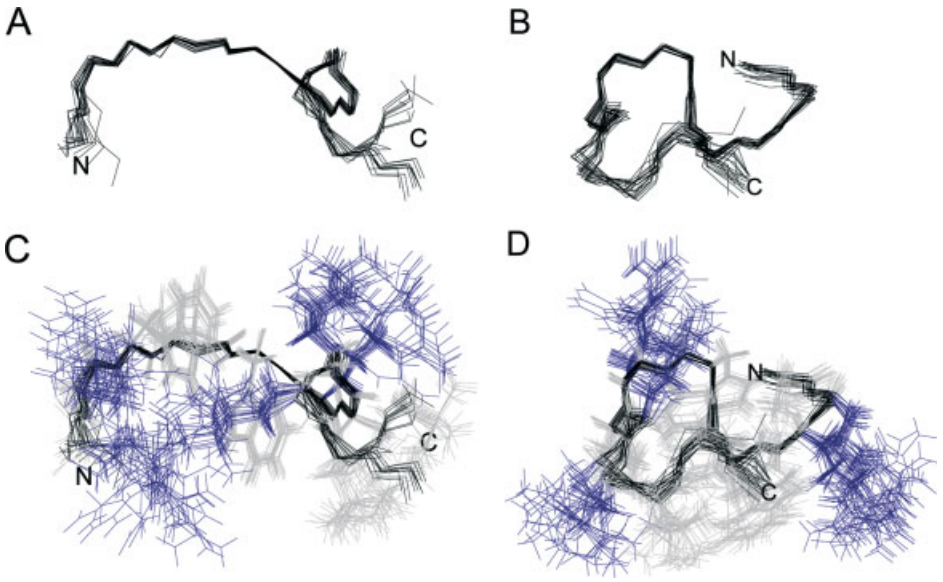

Figure 3 Final 20 lowest energy structures of LfcinB$_{4-14}$ and LfcinB$_{4-14}$Disu obtained in SDS micelles with residues 2–10 and 2–12, respectively, fitted to the mean structure. For LfcinB$_{4-14}$ and LfcinB$_{4-14}$Disu, respectively, (A) and (B) show the backbones while (C) and (D) show the backbones (black) with the side-chain bonds (positive side-chains in blue, remaining side-chains in grey). For LfcinB$_{4-14}$, the rmsd for backbone atoms is 0.577 Å and 1.025 Å for heavy atoms; for LfcinB$_{4-14}$Disu, rmsd for backbone atoms is 0.372 Å and 0.862Å for heavy atoms. The figures were generated using MOLMOL [50].

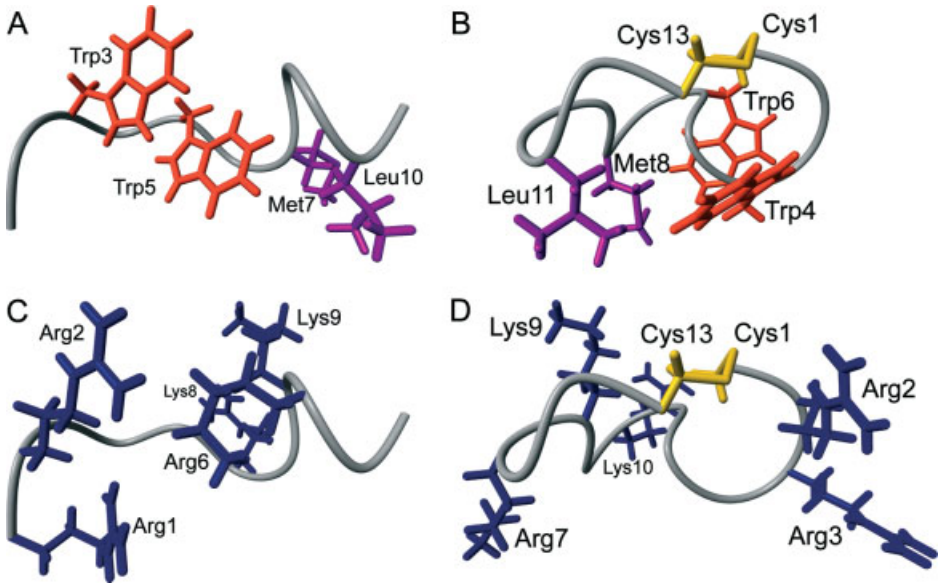

Figure 4 One of 20 lowest energy structures LfcinB$_{4-14}$ and LfcinB$_{4-14}$Disu, obtained in SDS micelles with residues 2–10 and 2–12, respectively, fitted to the mean structure. The backbones are in ribbon diagram representations, with neon representations of certain side-chains. For LfcinB$_{4-14}$ and LfcinB$_{4-14}$Disu, respectively, (A) and (B) show the hydrophobic Trp (orange), Met and Leu (purple) residues while (C) and (D) show the positive Lys and Arg (blue) residues in the same view. The figures were generated using MOLMOL [50].

conventional secondary structure in both peptides does not signify a lack of structural conformity because NOE crosspeaks found between the side-chains in the NMR spectra are definitely present, resulting in well-defined molecular structures. Like the linear peptide, the residues near the amidated *C*-terminus (residues 8–11) of the disulfide-linked structure have sharp backbone bends. Compared with LfcinB$_{4-14}$, the hydrophobic residues of LfcinB$_{4-14}$Disu are more segregated to one side of the peptide (Figure 4B). Another differing characteristic is the planar aromatic rings of Trp4 and Trp6 being almost perpendicular to each other. The positive residues still branch out from the peptide at various angles to form a positively

charged cloud around the peptide (Figure 4D), but these charged side-chains are less spread out than seen for the linear peptide. This makes LfcinB$_{4-14}$Disu a more amphipathic molecule.

DISCUSSION

LfcinB$_{4-14}$ has previously been reported to be similarly effective in its antimicrobial properties as the 25-residue LfcinB peptide [6]. The antimicrobial assays performed clarify this point by showing that its potent activity is preferential toward Gram-negative bacteria, represented by *E. coli*, over Gram-positive bacteria, represented by *S. aureus*. This preferred activity could be related to a previous finding of LfcinB binding interactions with lipoteichoic acid, which are generally found on the cell surface of Gram-positive bacteria and thought to be the initial negatively charged binding structures for the cationic peptide [17]. The introduction of a disulfide bond to make the cyclic counterpart, LfcinB$_{4-14}$Disu, results in a greater general antimicrobial efficiency while still being more inhibitory to *E. coli*. It is interesting to note that the short 6-residue antimicrobial active center of LfcinB as well as the full length LfcinB peptide, meanwhile, do not have different activities against *E. coli* and *S. aureus* [5]. Also, it is encouraging that the addition of the disulfide bond did not affect the non-hemolytic properties of LfcinB$_{4-14}$.

Calcein leakage assays showed that the vesicular membranes are not greatly permeated by the peptides studied under the experimental conditions; where tritrpticin causes dramatic leakage. In comparison, tritrpticin, which has similar antimicrobial potency to LfcinB$_{4-14}$Disu, showed a significantly increased degree of leakage. This suggests that the antimicrobial mechanism of LfcinB$_{4-14}$ and LfcinB$_{4-14}$Disu may not be via cell lysis. This finding agrees with a previous study [20] with *E. coli*, ruling out the antimicrobial mechanism of native LfcinB to be through direct cell lysis. An alternative mechanism of activity involves translocation of the peptide into the cell, where it may exert an intracellular effect. Such an effect could involve DNA binding, as Kanyshkova *et al.* [40] have shown that a 30 kDa *N*-terminal trypsin-digested product of human lactoferrin can bind non-specifically to DNA. Another possible intracellular antimicrobial effect could be the promotion of aggregate formations of unfolded proteins, including nascent proteins, as LfcinB has been shown to cause [41].

It has been found that membrane leakage induced by curvature-strain promoting peptides is greater in membranes containing PC in place of PE [42]. This result might explain the greater amount of calcein leaking that was seen with ePC : ePG LUVs over ePE : ePG LUVs, although, given the margin of error in these experiments, the differences are probably not significant.

Although the calcein leakage results suggest that the mode of action for these peptides is not on the bacterial membrane, this interaction remains important because the peptides still need to cross the membranes to get to an intracellular target. This conclusion is supported by an observed correlation between the cell-binding and lethal-activities of LfcinB [9]. Furthermore, our Trp fluorescence results show that there is little or no interaction between the LfcinB derived peptides and ePE : ePC LUVs which comprise neutral head groups as a membrane model for mammalian cells. The introduction of the anionic PG, a great component of most bacterial membranes, to make ePE : ePG and ePC : ePG LUVs allows for interactions with LfcinB$_{4-14}$ and LfcinB$_{4-14}$Disu. Therefore, even though the mode of action for these peptides is not localized to the membrane, peptide–lipid interactions remain a worthwhile topic of study because they seem to dictate specificity for the type of cell that is affected by these peptides.

The Trp residues of membrane proteins partition preferentially at the membrane interface [43–45], and so the extent of burial of the Trp residues in the bacterial membrane might help to explain the greater potency of the cyclic peptide over its linear analogue. To start with, the blue shifts found with the PG-containing LUVs prove that both peptides stay attached to the lipids, justifying our structural determination with the membrane mimetic SDS micelles. The greater hydrophobic environment surrounding the Trp residues of LfcinB$_{4-14}$Disu over LfcinB$_{4-14}$ may lead to the conclusion that the Trp residues of the disulfide-bonded peptide are entrenched deeper into the core of the bilayer. However, the Stern-Volmer constants from acrylamide quenching experiments indicate that the Trp residues of both peptides are almost equally protected from the accessible aqueous solvent, suggesting that the Trp residues of both peptides could be equally buried within the LUV bilayer. The greater blue shift found for LfcinB$_{4-14}$Disu could be attributed to the greater proximity of the Trp residues with the hydrophobic residues, Met8 and Leu11, than found for LfcinB$_{4-14}$. This is shown by comparing the NMR structures of both peptides (Figures 4A and 4B). On the other hand, it could be that, even though the Trp residues of both peptides are buried enough to be equally inaccessible to the soluble quencher, the Trp residues of LfcinB$_{4-14}$Disu are entrenched deeper into the bilayer and more exposed to the hydrophobic acyl tails of the lipids. Both of these two 'sources' of hydrophobicity probably play a part in explaining the blue shift results. Vesicle-bound LfcinB$_{4-14}$Disu has its Trp side chains within a closer distance to the Leu and Met residues than found for the extended peptide, and this greater hydrophobic side-chain clustering in turn

could promote deeper burial of the hydrophobic face of the peptide into the membrane.

The acrylamide quenching and blue shift findings with the detergent DPC led to concerns about its use for NMR studies with the LfcinB-derived peptides. $LfcinB_{4-14}Disu$ seems to have its Trp residues well entrenched in the DPC micelles. $LfcinB_{4-14}$ may be exposed almost as much to the hydrophobicity of the fatty acyl tails of the lipids as the disulfide-bonded counterpart, but the Trp residues of the linear peptide seem to interact with the region of the acyl chains that are closer to the head groups of the DPC molecules, as suggested by the lack of difference in acrylamide quenching efficiency found with the LUVs. In contrast, the SDS results show roughly the same amount of Trp burial for both peptides as the ePC : ePG and ePE : ePG vesicles. The data from these detergents justify performing the NMR studies of the peptides bound to SDS micelles over DPC.

The NMR structures presented depict how the Trp residues from $LfcinB_{4-14}Disu$ may interact more with hydrophobic surfaces than $LfcinB_{4-14}$. Looking at Figure 4B, the Trp, Leu and Met side-chains are closer to each other and lie on one side of the cyclized peptide, providing a better surface for hydrophobic interaction with lipids. Figure 4A of the 11-residue peptide shows that it only has its Met and Leu side-chains in close proximity to each other and protruding out of the main peptide. Trp5 of this peptide is found mostly on the interior of the backbone structure, with a small part of its aromatic ring jutting out into the same side as Met and Leu. Even further away from this hydrophobic grouping is Trp3. Although these four residues are on the same side, the greater spacing between them decreases the likeliness of a strong hydrophobic cluster to interact with the detergent acyl tail. It can be seen, then, that the Trp side-chains are not greatly buried. The hydrophobic cluster that comprises these four residues being packed closely on $LfcinB_{4-14}Disu$, on the other hand, supports the deeper burial of the Trp residues suggested by the fluorescence results.

The structure of the full length 25-residue LfcinB peptide [47] shows that it has a great degree of amphipathicity, where the majority of positive charges on LfcinB are positioned outside the main hydrophobic cluster of the peptide. This amphipathic character is also seen in the 13-residue $LfcinB_{4-14}Disu$ peptide, albeit to a lesser degree. Due to the less extended cyclic backbone, the positive charges are more spread out between each other than in the linear peptide (Figure 4D). In addition, these Lys and Arg side-chains adopt a greater variety of conformations between each of the 20 final calculated structures which, when overlaid on top of each other, makes an electropositive cloud around a portion of the peptide. On the hydrophobic side, a tight cluster was found on one side of $LfcinB_{4-14}Disu$, whereas on $LfcinB_{4-14}$, the hydrophobic residues were further spaced away from each other. Amphipathicity allows for the positive charges of the peptide to be attracted electrostatically to the membrane surface, and then allows the hydrophobic cluster to interact with membrane lipid tails to secure binding [48]. In accordance with the notion that the Trp amino acids of Lfcin direct it to bind to the interface of the membrane [16], the outlying Arg and Lys residues of the peptide structures could interact with hydrophilic components of a membrane while the Trp residues, which actually comprise both a hydrophobic and a hydrophilic character, could be found near the membrane surface as seen in most membrane proteins [44].

The loss of regular secondary structure in these two peptides from a ß-sheet found in intact LfcinB that is thought to promote the amphipathicity of the peptide [47] is not surprising given the shorter sequence of these peptides. This loss of the ß-sheet was also found for the active hexamer when the latter is bound to membrane mimetic surfaces [49].

In terms of the *in vivo* applicability of the peptides, the more defined NMR structure for the entire sequence of $LfcinB_{4-14}Disu$ over $LfcinB_{4-14}$ suggests that the disulfide link confers additional stability. This conclusion makes particular sense given that the *C*-terminal residue of $LfcinB_{4-14}$ is a small glycine, making its conformation susceptible to surrounding conditions. The hydrophobic residues of the $LfcinB_{4-14}Disu$ are closer to each other than in the smaller peptide, possibly giving a greater stability for hydrophobic interactions. However, the success in designing a more stable molecule is somewhat offset by the added constraints given by the cyclic quality of the peptide, with less residues being in the most favored group of the Ramachandran map [37].

In designing a new peptide based on the 11-residue stretch of LfcinB that provides an optimal balance of antibacterial activity and safety to mammalian cells, the studies here show that the disulfide-linked and *C*-terminus amidated peptide gives greater antimicrobial potency than the linear 11-residue peptide. Membrane disruption caused by these peptides was low, but membrane interactions remain important to explain the antimicrobial action of these peptides. Spectroscopic studies using fluorescence and NMR show deeper insertion of the Trp residues into the membrane. Solution NMR structures of SDS micelle bound peptide also show in both peptides the formation of a cloud of positive residues covering much of the peptide except for a hydrophobic cluster, giving the peptide a greater amphipathic character.

Acknowledgements

The authors would like to thank Ø. Rekdal and his coworkers at the University of Tromsø, Tromsø,

Norway, for performing the antibacterial and hemolytic assays. We are indebted to Dr Howard Hunter for many suggestions and to Dr Deane MacIntyre for management and upkeep of the NMR facilities. Maintenance of the NMR facility is supported by the Canadian Institutes for Health Research. The BioNMR Centre was recently upgraded with funds provided by the Canada Foundation for Innovation, the Alberta Science and Research Authority and the Alberta Heritage Foundation for Medical Research.

The atomic coordinates and structure factors (codes 1Y58 (LfcinB$_{4-14}$Disu) and 1Y58 (LfcinB$_{4-14}$)) have been deposited in the Protein Data Bank, Research Collaboratory for Structural Bioinformatics, Rutgers University, New Brunswick, NJ, (http://www.rcsb.org/).

REFERENCES

1. Masson PL, Heremans JF, Dive CH. An iron binding protein common to many external secretions. *Clin. Chim. Acta* 1966; **14**: 735–739.
2. Bellamy WR, Takase M, Yamauchi K, Wakabayashi H, Kawase K, Tomita M. Identification of the bactericidal domain of lactoferrin. *Biochim. Biophys. Acta* 1992; **1121**: 130–136.
3. Strom MB, Haug BE, Rekdal Ø, Skar ML, Stensen W, Svendsen JS. Important structural features of 15-residue lactoferricin derivatives and methods for improvement of antimicrobial activity. *Biochem. Cell Biol.* 2002; **80**: 65–74.
4. Vorland LH, Ulvatne H, Andersen J, Haukland HH, Rekdal Ø, Svendsen JS, Gutteberg TJ. Lactoferricin of bovine origin is more active than lactoferricins of human, murine and caprine origin. *Scand. J. Infect. Dis.* 1998; **30**: 513–517.
5. Tomita M, Takase M, Bellamy W, Shimamura S. A review: the active peptide of lactoferrin. *Acta Paediatr. Jpn* 1994; **36**: 585–591.
6. Kang JH, Lee MK, Kim KL, Hahm K-S. Structure-biological activity relationships of 11-residue highly basic peptide segment of bovine lactoferrin. *Int. J. Pept. Protein Res.* 1996; **48**: 357–363.
7. Haug BE, Svendsen JS. The role of tryptophan in the antibacterial activity of a 15-residue bovine lactoferricin peptide. *J. Pept. Sci.* 2001; **7**: 190–196.
8. Hancock RE, Chapple DS. Peptide antibiotics. *Antimicrob. Agents Chemother.* 1999; **43**: 1317–1328.
9. Bellamy WR, Wakabayashi H, Takase M, Kawase K, Shimamura S, Tomita M. Role of cell-binding in the antibacterial mechanism of lactoferricin B. *J. Appl. Bact.* 1993; **75**: 478–484.
10. Hoek KS, Milne JM, Grieve PA, Dionysius DA, Smith R. Antibacterial activity in bovine lactoferrin-derived peptides. *Antimicrob. Agents Chemother.* 1997; **41**: 54–59.
11. Rozek A, Powers JP, Friedrich CL, Hancock RE. Structure-based design of an indolicidin peptide analogue with increased protease stability. *Biochemistry* 2003; **42**: 14 130–14 138.
12. Boman HG. Peptide antibiotics and their role in innate immunity. *Annu. Rev. Immunol.* 1995; **13**: 61–92.
13. Park CB, Yi KS, Matsuzaki K, Kim HS, Kim SC. Structure-activity analysis of buforin II, a histone H2A-derived antimicrobial peptide: the proline hinge is responsible for the cell-penetrating ability of buforin II. *Proc. Natl Acad. Sci. USA* 2000; **97**: 8245–8250.
14. Epand RM, Vogel HJ. Diversity of antimicrobial peptides and their mechanisms of action. *Biochim. Biophys. Acta* 1999; **1462**: 11–28.
15. Hancock RE, Rozek A. Role of membranes in the activities of antimicrobial cationic peptides *FEMS Microbiol. Lett.* 2002; **206**: 143–149.
16. Vogel HJ, Schibli DJ, Jing W, Lohmeier-Vogel EM, Epand RF, Epand RM. Towards a structure-function analysis of bovine lactoferricin and related tryptophan- and arginine-containing peptides. *Biochem. Cell Biol.* 2002; **80**: 49–63.
17. Vorland LH, Ulvatne H, Andersen J, Haukland HH, Rekdal Ø, Svendsen JS, Gutteberg TJ. Antimicrobial effects of lactoferricin B. *Scand. J. Infect. Dis.* 1999; **31**: 179–184.
18. Brewer D, Lajoie G. Structure-based design of potent histatin analogues. *Biochemistry* 2002; **41**: 5526–5536.
19. Wang S-W. p-Alkoxybenzyl alcohol resin and p-alkoxybenzyloxy-carbonylhydrazide resin for solid phase synthesis of protected peptide fragments. *J. Am. Chem. Soc.* 1973; **95**: 1328–1333.
20. Ulvatne H, Haukland HH, Olsvik Ø, Vorland LH. Lactoferricin B causes depolarization of the cytoplasmic membrane of *Escherichia coli* ATCC 25 922 and fusion of negatively charged liposomes. *FEBS Lett.* 2001; **492**: 62–65.
21. Strom MB, Rekdal Ø, Svendsen JS. The effects of charge and lipophilicity on the antibacterial activity of undecapeptides derived from bovine lactoferricin. *J. Pept. Sci.* 2002; **8**: 36–43.
22. Schibli DJ, Epand RF, Vogel HJ, Epand RM. Tryptophan-rich antimicrobial peptides: comparative properties and membrane interactions. *Biochem. Cell Biol.* 2002; **80**: 667–677.
23. Eliassen LT, Berge G, Sveinbjornsson B, Svendsen JS, Vorland LH, Rekdal Ø. Evidence for a direct antitumor mechanism of action of bovine lactoferricin. *Anticancer Res.* 2002; **22**: 2703–2710.
24. Mosmann TR, Cherwinski H, Bond MW, Giedlin MA, Coffman RL. Two types of murine helper T cell clone. I. Definition according to profiles of lymphokine activities and secreted proteins. *J. Immunol.* 1986; **136**: 2348–2357.
25. Mayer LD, Hope MJ, Cullis PR. Vesicles of variable size produced by a rapid extrusion procedure. *Biochim. Biophys. Acta* 1986; **858**: 161–168.
26. Olson F, Hunt CA, Szoka EC, Vail WJ, Papahadjopoulos D. Preparation of liposomes of defined size distribution by extrusion through polycarbonate membranes. *Biochim. Biophys. Acta* 1979; **557**: 9–23.
27. Ames BN. Assay of inorganic phosphate, total phosphate and phosphatases. In *Methods in Enzymology*, Neufeld EF, Ginsberg V (eds). Academic Press: New York, 1966; 115–118.
28. Matsuzaki K, Fukui M, Fujii N, Miyajima K. Interactions of an antimicrobial peptide, tachyplesin I, with lipid membranes. *Biochim. Biophys. Acta* 1991; **1070**: 259–264.
29. Lakowicz JR. *Principles of Fluorescence Spectroscopy*. Kluwer Academic: New York, 1999.
30. Callihan D, West J, Kumar S, Schweitzer BI, Logan TM. Simple, distortion-free homonuclear spectra of peptides and nucleic acids in water using excitation sculpting. *J. Magn. Reson.* 1996; **B112**: 82–85.
31. Piotto M, Saudek V, Sklenar V. Gradient-tailored excitation for single-quantum NMR spectroscopy of aqueous solutions. *J. Biol. NMR* 1992; **2**: 661–665.
32. Delaglio F, Grzesiek S, Vuister G, Zhu G, Pfeifer J, Bax A. NMRPipe: a multidimensional spectral processing system based on UNIX Pipes. *J. Biomol. NMR* 1995; **6**: 277–293.
33. Johnson BA, Blevins RA. NMRView: A computer program for the visualization and analysis of MR data. *J. Biomol. NMR* 1994; **4**: 603–614.
34. Wüthrich K. *NMR of Proteins and Nucleic Acids*. Wiley: New York, 1986.
35. Brunger AT, Adams PD, Clore GM, DeLano WL, Gros P, Grosse-Kunstleve RW, Jiang J-S, Kuszewski J, Nilges M, Pannu NS, Read RJ, Rice LM, Simonson T, Warren GL. Crystallography and NMR system (CNS): A new software system for macromolecular structure determination. *Acta Crystallogr.* 1998; **D54**: 905–921.
36. Linge JP, Nilges M. Influence of non-bonded parameters on the quality of NMR structures: a new force field for NMR structure calculation. *J. Biomol. NMR* 1999; **13**: 51–59.
37. Petruska JA, Hodge AJ. Recent studies with the electron microscope on ordered aggregates of the tropocollagen molecule. In *Aspects of Protein Structure*, Ramachandran GN (ed.). Academic Press: New York, 1963; 289–300.

38. Laskowski RA, Rullmannn JA, MacArthur MW, Kaptein R, Thornton JM. AQUA and PROCHECK-NMR: programs for checking the quality of protein structures solved by NMR. *J. Biomol. NMR* 1996; **8**: 477–486.
39. Pavone V, Gaeta G, Lombardi A, Nastri F, Maglio O, Isernia C, Saviano M. Discovering protein secondary structures: Classification and description of isolated α-turns. *Biopolymers* 1996; **38**: 705–721.
40. Kanyshkova TG, Semenov DV, Buneva VN, Nevinsky GA. Human milk lactoferrin binds two DNA molecules with different affinities. *FEBS Lett.* 1999; **451**: 235–237.
41. Takase K. Reactions of denatured proteins with other cellular components to form insoluble aggregates and protection by lactoferrin. *FEBS Lett.* 1998; **441**: 271–274.
42. Matsuzaki K, Sugishita K, Ishibe N, Ueha M, Nakata S, Miyajima K, Epand RM. Relationship of membrane curvature to the formation of pores by magainin 2. *Biochemistry* 1998; **37**: 11 856–11 863.
43. Kachel K, Asuncion-Punzalan E, London E. Anchoring of tryptophan and tyrosine analogs at the hydrocarbon-polar boundary in model membrane vesicles: parallax analysis of fluorescence quenching induced by nitroxide-labeled phospholipids. *Biochemistry* 1995; **34**: 15 475–15 479.
44. Morein S, Strandberg E, Kilhan JA, Persson S, Arvidon G, Koeppe RE, Lindblom G. Influence of membrane-spanning α-helical peptides on the phase behavior of the dioleoylphosphatidylcholine/water system. *Biophys. J.* 1997; **73**: 3078–3088.
45. Reithmeier RA. Characterization and modeling of membrane proteins using sequence analysis. *Curr. Opin. Struct. Biol.* 1995; **5**: 491–500.
46. Yau WM, Wimley WC, Gawrisch K, White SH. The preference of tryptophan for membrane interfaces. *Biochemistry* 1998; **37**: 14 712–14 718.
47. Hwang PM, Zhou N, Shan X, Arrowsmith CH, Vogel HJ. Three-dimensional solution structure of lactoferricin B, an antimicrobial peptide derived from bovine lactoferrin. *Biochemistry* 1998; **37**: 4288–4298.
48. Schibli DJ, Vogel HJ. Structural studies of lactoferricin B, and its antimicrobial active peptide fragments. In *Structure, Function and Applications*, Shimazaki K (ed.). Elsevier Press: New York, 2000; 27–35.
49. Schibli DJ, Hwang PM, Vogel HJ. Structure of the antimicrobial active center of lactoferricin B bound to sodium dodecyl sulfate micelles. *FEBS Lett.* 1999; **446**: 213–217.
50. Koradi R, Billeter M, Wüthrich K. MOLMOL: a program for display and analysis of macromolecular structures. *J. Mol. Graph.* 1996; **14**: 29–32.